



## TOPOLOGY OPTIMIZATION OF PLANE STRUCTURES USING BINARY LEVEL SET METHOD AND ISOGEOMETRIC ANALYSIS

M. Khatibinia<sup>1\*,†</sup>, M. Roodsarabi<sup>1</sup> and M. Barati<sup>2</sup>

<sup>1</sup>*Department of Civil Engineering, University of Birjand, Birjand, Iran*

<sup>2</sup>*Department of Civil Engineering, Ferdowsi University of Mashhad, Mashhad, Iran*

### ABSTRACT

This paper presents the topology optimization of plane structures using a binary level set (BLS) approach and isogeometric analysis (IGA). In the standard level set method, the domain boundary is described as an isocountour of a scalar function of a higher dimensionality. The evolution of this boundary is governed by Hamilton–Jacobi equation. In the BLS method, the interfaces of subdomains are implicitly represented by the discontinuities of BLS functions taking two values 1 or  $-1$ . The subdomains interfaces are represented by discontinuities of these functions. Using a two–phase approximation and the BLS approach the original structural optimization problem is reformulated as an equivalent constrained optimization problem in terms of this level set function. For solving drawbacks of the conventional finite element method (FEM), IGA based on a Non–Uniform Rational B–Splines (NURBS) is adopted to describe the field variables as the geometry of the domain. For this purpose, the B–Spline functions are utilized as the shape functions of FEM for analysis of structure and the control points are considered the same role with nodes in FEM. Three benchmark examples are presented to investigate the performance the topology optimization based on the proposed method. Numerical results demonstrate that the BLS method with IGA can be utilized in this field.

**Keywords:** topology optimization; isogeometric analysis; binary level set method; Non–Uniform Rational B–Splines.

Received: 25 July 2017; Accepted: 15 August 2017

### 1. INTRODUCTION

The solution of optimal topology design problems is very important and challenging in science and computational engineering [1]. Topology optimization approach has been

---

\*Corresponding author: Department of Civil Engineering, University of Birjand, Birjand, Iran

†E-mail address: m.khatibinia@birjand.ac.ir (M. Khatibinia)

extensively utilized to a variety of structural optimization problems such as the stiffness maximization problem, vibration problems, optimum design problems for compliant mechanisms, and thermal problems. In the topology optimization approach, the main aim is to find the geometry of a design in terms of shape and topology to perform a specific task optimally, ranging from discrete gridlike structures to continuum structures [2, 3]. In contrast to the detailed designs (e.g. size and shape optimizations) of a structure, topology optimization does not require a close-to-optimal initial design and is able to generate optimal geometries when intuitive design approaches fail, e.g., due to complex interdependencies between design parameters and the structural response. A number of methods such as Optimality Criteria (OC) methods [4, 5], the approximation methods [6–9], the Method of Moving Asymptotes (MMA) [9–11], Evolutionary Structural Optimization (ESO) method [12] and even more heuristic methods such as genetic algorithm [13] and ant colony [14] have been proposed for solving the topology optimization problems.

In recent years, the level set method (LSM) originally proposed by Osher and Sethian [15] has been adopted as a new technique to utilize in optimizing shape and topology of structures [16–21]. In the LSM, the boundaries of design domain are implicitly represented by the zero level set of a higher dimensional function. The standard LSM requires for solving Hamilton–Jacobi Partially Differential Equation (H–J PDE). This causes several limitations such as re-initialization process, the Courant–Friedrichs–Lewy (CFL) condition and dependency of final design to initial guess. To overcome these drawbacks several LSMs have been proposed [13–23]. The binary level set method (BLSM) has been proposed as a new approach of the LSM [22–24]. Distinct from the conventional LSM, interfaces are represented by the discontinuous locations of the binary level set (BLS) functions with only two values 1 and  $-1$  at convergence. The BLSMs is closely related to the phase-field method, which has been applied for the image processing [25] and topology optimization [24, 26].

By recent developments in the Computer Aided Geometry Design (CAGD) technology, the geometrical definition and generation of complex surfaces and objects have become achievable [27]. In order to achieve this purpose, Splines and some modified versions of them, i.e. Non-Uniform Rational B-Splines (NURBS) and T-Splines, are commonly utilized. In the development of advanced computational methodologies, Hughes *et al.* [27] proposed a Non-Uniform Rational B-Splines (NURBS)-based isogeometric analysis (IGA) to eliminate the gap between CAGD and finite element analysis. In contrast to the standard finite element method (FEM) with Lagrange polynomial basis, the IGA approach utilizes more general basis functions such as NURBS that are common in CAD approaches. Thus, IGA is very promising because it can directly use CAD data to describe both exact geometry and approximate solution.

The present study presents is the topology optimization of plane structures using the BLSM with IGA. In order to achieve this purpose, the BLSM is firstly utilized to solve the topology optimization problem. Then, IGA based on NURBS is applied to describe the field variables as the geometry of the domain. In the IGA approach, control points is considered as the same role with nodes in FEM and B-Spline basis functions are utilized as shape functions of FEM for analysis of structure. Three benchmark examples are presented to illustrate the validity of the proposed method. The optimal results demonstrate that the BLSM with IGA can be considered as a efficient topology optimization method in the topology optimization of plane structures.

## 2. MATHEMATICAL FORMULATION OF TOPOLOGY OPTIMIZATION

In the present study, a plane structure with the linear property of material is constructed for defining the problem of topology optimization. In this problem,  $\Omega \subseteq \mathbf{R}^n$  is assumed an open and bounded set occupied by a linear isotropic elastic structure. The boundary of  $\Omega$  consists of three parts  $\Gamma = \partial\Omega = \Gamma_d \cup \Gamma_u \cup \Gamma_t$ , with Dirichlet boundary conditions on  $\Gamma_u$  and Neumann boundary conditions on  $\Gamma_t$ . Furthermore,  $\Gamma_d$  is traction free. The displacement field in  $\Omega$  is the unique solution of the linear elastic system and is expressed as [28]:

$$\begin{cases} -\text{div } \sigma(u) = p & \text{in } \Omega \\ u = u_0 & \text{in } \Gamma_u \\ \sigma(u) \cdot N = \tau & \text{in } \Gamma_t \end{cases} \quad (1)$$

where  $u$  is the nodal displacement field function. The strain tensor  $\varepsilon$  and the stress tensor  $\sigma$  at any point  $\Omega$  are defined in the usual form as:

$$\begin{cases} \sigma_{ij}(u) = E_{ijkl} \varepsilon_{kl}(u) \\ \varepsilon_{ij}(u) = \frac{1}{2} \left( \frac{\partial u_i}{\partial x_j} + \frac{\partial u_j}{\partial x_i} \right) \end{cases} \quad (2)$$

where  $E_{ijkl}$  is the elasticity tensor; and  $\varepsilon_{ij}$  is the liberalized strain tensor.

The main aim of the topology optimization is to find a suitable shape in the admissible design space, so that the objective functional can obtain its minimum or at least a local minimum. Therefore, this can be expressed as follows [30, 31]:

$$\begin{aligned} \text{Minimize: } & J(u) = \int_{\Omega} F(u) d\Omega \\ \text{Subject to: } & \int_{\Omega} E_{ijkl} \varepsilon_{ij}(u) \varepsilon_{kl}(v) d\Omega = \int_{\Omega} p v d\Omega + \int_{\Gamma_t} \tau v d\Gamma \quad \text{for all } v \in U \\ & u = u_0 \quad \text{on } \Gamma_u \\ & Vol = \int_{\Omega} d\Omega \leq V_{\max} \end{aligned} \quad (3)$$

where  $v$  is the adjoint displacement field function in the space  $U$  of kinematically admissible displacement fields. Field function  $u_0$  prescribes displacement field on partial boundary  $\Gamma_u$ .  $p$  is the body force.  $\tau$  is the boundary traction. The inequality describes the limit on the amount of material in terms of the maximum admissible volume  $V_{\max}$  of the design domain.

## 3. STANDARD LEVEL SET METHOD FOR TOPOLOGY OPTIMIZATION

The standard level set method (LSM) developed by Osher and Sethian [30] can be referred

to as implicit moving boundary models. In this method, the boundary of structure is described by zero level set and can easily represent complicated surface shapes that can form holes, split to form multiple boundaries, or merge with other boundaries to form a single surface. Based on the concept of propagation of the level set surface, the design changes are carried out to solve the problem of structural topology optimization. Therefore, these definitions are also defined as follows [30]:

$$\begin{cases} \phi(x) < 0 : \forall x \in \Omega / \bar{\Omega} \\ \phi(x) = 0 : \forall x \in \partial\Omega \\ \phi(x) > 0 : \forall x \in \Omega \setminus \partial\Omega \end{cases} \quad (4)$$

The implicit function  $\phi(x)$  is used to represent the boundary and to optimize it, as it was originally developed for curve and surface evolution. The change of the implicit function  $\phi(x)$  is governed by the simple convection equation as:

$$\frac{\partial\phi(x,t)}{\partial t} + \nabla\phi(x,t) \cdot V(x) = 0 \quad (5)$$

where  $V(x)$  defines the velocity of each point on the boundary. The parameter  $t$  is a fictitious time parameter that represents the optimization iteration number, and the time step,  $t$ , is chosen in such away that the Courant–Friedrichs–Lewy (CFL) condition is satisfied [17]. Since the tangential components of  $V$  would vanish, it can be written as:

$$\frac{\partial\phi(x,t)}{\partial t} + V_N |\nabla\phi(x,t)| = 0 \quad (6)$$

where  $V_N$  is the normal velocity.

These two H–J PDEs are the well-known level set equations. Solving H–J PDE causes several limitations such as re-initialization process, the Courant–Friedrichs–Lewy (CFL) condition and dependency of final design to initial guess. Hence, the binary level set method (BLSM) was proposed by Lie *et al.* [22] in order to eliminate the drawbacks of the standard LSM.

#### 4. THE BINARY LEVEL SET METHOD

In this section, the formulation of BLSM is first presented and then apply BLSM for the structural topology optimization.

##### 4.1 Basic formulations of BLSM

In the BLSM, the subdomains are defined by the discontinuous level set functions which take the values 1 and  $-1$  at convergence. The representation of two domains  $(\Omega_1, \Omega_2)$  can be

given as follows [22]:

$$\phi(x) = \begin{cases} 1 & \forall x \in \Omega_1 \\ k & \forall x \in \Gamma \\ -1 & \forall x \in \Omega_2 \end{cases} \quad (7)$$

where  $k \in (-1, 1)$ . A piecewise constant function  $\rho(x)$  that equals to  $c_1$  in  $\Omega_1$ , and  $c_2$  in  $\Omega_2$  then  $\rho(x)$  can be expressed as [22]:

$$\rho(x) = \frac{1}{2} [c_1(\phi + 1) + c_2(1 - \phi)] \quad (8)$$

More generally, using  $N$  BLS functions  $\{\phi_i\}_{i=1}^N$ ,  $2^N$  subdomains  $\{\phi_i\}_{i=1}^{2^N}$  can be represented. By introducing the vectors  $\Phi = \{\phi_1, \phi_2, \dots, \phi_N\}$  and  $\mathbf{c} = \{c_1, c_2, \dots, c_N\}$ . For  $i = 1, 2, \dots, 2^N$ , let  $(b_1^{i-1}, b_2^{i-1}, \dots, b_N^{i-1})$  be the binary representation of  $i-1$ , i.e.,  $b_j^{i-1} = 0$  or  $1$ . Also, it is defined,

$$s(i) = \sum_{j=1}^N b_j^{i-1} \quad (9)$$

and write characteristic function  $\psi_i$  as the product

$$\psi_i = \frac{(-1)^{s(i)}}{2^N} \prod_{j=1}^N (\phi_j + 1 - 2b_j^{i-1}) \quad (10)$$

Therefor, the piecewise constant function can be represented as:

$$\rho = \sum_{i=1}^{2^N} c_i \psi_i \quad (11)$$

In order to ensure the BLS functions converges to values 1 and -1 at every point in  $\Omega$ , these functions are required to satisfy  $K(\phi) = \phi_i^2 - 1 = 0$  for  $i = 1, 2, \dots, N$ . Furthermore, the volume and the perimeter of each subdomain are calculated with the following formulation:

$$|\Omega_i| = \int_{\Omega} \psi_i dx \quad ; \quad |\partial\Omega_i| = \int_{\Omega} |\nabla \psi_i| dx \quad (12)$$

#### 4.2 BLSM for the structural topology optimization

In this section, the formulation of BLSM is described for solving the topology optimization problem of plane structures. In order to achieve this purpose, the piecewise constant density

function based on Equation (8) is defined as follows [26]:

$$\rho(x) = \frac{1}{2} [c_1(1-\phi) + c_2(1+\phi)] \quad (13)$$

where  $c_1$  and  $c_2$  are constant and are set to  $-1$  and  $+1$ , respectively. In fact,  $c_1 = -1$  and  $c_2 = 1$  indicate the hole and no hole in the topology of structure, respectively.

In this study, the main aim of the topology optimization is to minimize the compliance over the structural domain for general loading condition and several constraints. Hence, the formulation of topology optimization based on BLSM is expressed as follows [26]:

$$\begin{aligned} \text{Minimize: } & J(u, \phi) = \int_{\Omega} \rho(\phi) F(u) d\Omega + \beta \int_{\Omega} |\nabla \phi| d\Omega \\ \text{Subjet to: } & H_1 = \int_{\Omega} \rho(\phi) dx - V_{\max} \leq 0 \\ & H_2 = K(\phi) = 0 \\ & a(u, v, \phi) = l(v, \phi) \\ \text{for all: } & v \in U, \quad u|_{\Gamma_D} = u_0 \end{aligned} \quad (14)$$

where

$$\begin{aligned} a(u, v, \phi) &= \int_{\Omega} \rho(\phi) E_{i,j,k,l} \varepsilon_{i,j}(u) \varepsilon_{k,l}(v) d\Omega \\ l(v, \phi) &= \int_{\Omega} f \cdot v d\Omega + \int_{\Gamma_N} g \cdot v d\Gamma \end{aligned} \quad (15)$$

In the objective function defined in Equation (14),  $F(u) = 1/2 E_{i,j,k,l} \varepsilon_{i,j}(u) \varepsilon_{k,l}(u)$  is the strain energy density, and  $\rho$  is the material density ratio. The second term in the objective function is the regularization term and  $\beta$  is a nonnegative value to control the effect of this term.  $H_1$  indicates the material fraction for different phases, and  $H_2$  is the piecewise constant constraint to guarantee LSF which belongs to only one phase. Using the augmented Lagrangian method, the optimization problem i.e., Equation (14) can be converted into an unconstrained problem as:

$$L(\phi, \lambda) = J(\phi) - a(u, v, \phi) + l(\phi, \lambda) + \lambda_1 H_1 + \frac{1}{2\mu_1} H_1^2 + \lambda_2 \int_{\Omega} H_2 d\Omega + \frac{1}{2\mu_2} \int_{\Omega} H_2^2 d\Omega \quad (16)$$

where  $\lambda_1 \in R$  and  $\lambda_2 \in L^2(\Omega)$  are Lagrange multiplier, and  $\mu_1, \mu_2 > 0$  are penalty parameters.

The saddle point of this function i.e., Equation (16), can be obtained by the following formulation which was proposed by Wei and Wang [32]:

$$\int_{\Omega} \Psi(u, \phi, \tilde{\lambda}_1, \tilde{\lambda}_2) \partial \phi d\Omega = 0 \quad (18)$$

$$\Psi(u, \phi, \tilde{\lambda}_1, \tilde{\lambda}_2) = \frac{1}{2} \rho'(\phi) E_{i,j,k,l} \varepsilon_{i,j}(u) \varepsilon_{k,l}(u) + \beta \nabla \cdot \left( \frac{\nabla \phi}{|\nabla \phi|} \right) + \tilde{\lambda}_1 \rho'(\phi) + \tilde{\lambda}_2 K'(\phi) \quad (19)$$

where

$$\rho'(\phi) = \frac{\partial \rho(\phi)}{\partial \phi} = \frac{1}{2} (c_2 - c_1) \quad (20)$$

$$K'(\phi) = \frac{\partial K(\phi)}{\partial \phi} = 2\phi \quad (21)$$

and

$$\tilde{\lambda}_1 = \lambda_1 + \frac{1}{\mu_1} \left( \int_{\Omega} \rho(\phi) d\Omega - V_0 \right) \quad (22)$$

$$\tilde{\lambda}_2 = \lambda_2 + \frac{1}{\mu_2} K(\phi) \quad (23)$$

In order to satisfy Equation (18), the steepest descent method was proposed as [32]:

$$\frac{d\phi}{dt} = -\psi, \quad \phi^0 = \phi_0 \quad (24)$$

According to the previous formulation, the problem of the structural topology optimization is converted into an ordinary differential problem with initial value  $\phi_0$ . A semiimplicit method with the additive operator splitting (AOS) scheme [33, 34] is utilized for solving Equation (24). For updating Lagrange multipliers  $\lambda_1$  and penalty parameters  $\mu_1$ , the following equations are employed as,

$$\begin{aligned} \lambda_1^{k+1} &= \lambda_1^k + \frac{1}{\mu_1^k} \left( \int_{\Omega} \rho(\phi) d\Omega - V_0 \right) \\ \lambda_2^{k+1} &= \lambda_2^k + \frac{1}{\mu_2^k} K(\phi) \\ \mu_i^{k+1} &= \alpha \mu_i^k \quad ; \quad i = 1, 2 \end{aligned} \quad (25)$$

## 5. ISOGEOMETRIC FINITE ELEMENTS

In this section, a short overview is given on the main features of isogeometric finite elements and is applied for the static analysis of a plane structure.

### 5.1 Surface definition by NURBS basis function

A surface based on NURBS can parametrically defined as [21, 27]:

$$S(\xi, \eta) = \frac{\sum_{i=1}^n \sum_{j=1}^m N_{i,p}(\xi) N_{j,q}(\eta) \omega_{i,j} P_{i,j}}{\sum_{i=1}^n \sum_{j=1}^m N_{i,p}(\xi) N_{j,q}(\eta) \omega_{i,j}} \quad (26)$$

where  $P_{i,j}$  are  $(n, m)$  control points,  $\omega_{i,j}$  are the associated weights and  $N_{i,p}(\xi)$  and  $N_{j,q}(\eta)$  are the normalized B-splines basis functions of degree  $p$  and  $q$  respectively. The  $i$ th B-spline basis function of degree  $p$ , denoted by  $N_{i,p}(\xi)$ , is defined recursively as:

$$N_{i,0}(\xi) = \begin{cases} 1 & \text{if } \xi_i \leq \xi < \xi_{i+1} \\ 0 & \text{otherwise} \end{cases} \quad (27)$$

and

$$N_{i,p}(\xi) = \frac{\xi - \xi_i}{\xi_{i+p} - \xi_i} N_{i,p-1}(\xi) + \frac{\xi_{i+p+1} - \xi}{\xi_{i+p+1} - \xi_{i+1}} N_{i+1,p-1}(\xi) \quad (28)$$

where  $\xi = \{\xi_0, \xi_1, \dots, \xi_r\}$  is the knot vector and,  $\xi_i$  are a non-decreasing sequence of real numbers, which are called knots. The knot vector  $\eta = \{\eta_0, \eta_1, \dots, \eta_s\}$  is employed to define the  $N_{j,q}(\eta)$  basis functions for other direction. The interval  $[\xi_0, \xi_r] \times [\eta_0, \eta_s]$  forms a patch [21]. A knot vector, for instance in  $\xi$  direction, is called open if the first and last knots have a multiplicity of  $p+1$ . In this case, the number of knots is equal to  $r = n + p$ . Also, the interval  $[\xi_i, \xi_{i+1})$  is called a knot span where at most  $p+1$  of the basis functions  $N_{i,p}(\xi)$  are non-zero which are  $N_{i-p,p}(\xi), \dots, N_{i,p}(\xi)$ .

### 5.2 Numerical formulation for plane elasticity structures

By using the NURBS basis functions for a patch  $p$ , the approximated displacement functions  $\mathbf{u}^p = [u, v]$  can be expressed as [21, 27]:

$$u^p(\xi, \eta) = \sum_{i=1}^n \sum_{j=1}^m R_{i,j}(\xi, \eta) u_{i,j}^p \quad (29)$$



where  $R_{i,j}(\xi, \eta)$  is the rational term in Equation (17). Furthermore, the geometry is approximated by B-spline basis functions as [27]:

$$S^p(\xi, \eta) = \sum_{i=1}^n \sum_{j=1}^m R_{i,j}(\xi, \eta) S_{i,j}^p \quad (30)$$

By using the local support property of NURBS basis functions, Equations (20) and (21) can be summarized as it follows in any given  $(\xi, \eta) \in [\xi_i, \xi_{i+1}] \times [\eta_j, \eta_{j+1}]$ .

$$u^p(\xi, \eta) = (u^p(\xi, \eta), v^p(\xi, \eta)) = \sum_{k=i-p}^i \sum_{l=j-q}^j R_{k,l}(\xi, \eta) U_{k,l}^p = \mathbf{R}\mathbf{U} \quad (31)$$

$$S^p(\xi, \eta) = (x^p(\xi, \eta), y^p(\xi, \eta)) = \sum_{k=i-p}^i \sum_{l=j-q}^j R_{k,l}(\xi, \eta) P_{k,l}^p = \mathbf{R}\mathbf{P} \quad (32)$$

The strain-displacement matrix  $\mathbf{B}$  can be constructed from the following fundamental equations,

$$\mathcal{E} = \mathbf{D}\mathbf{u}^p = \mathbf{B}(\xi, \eta)\mathbf{u}^p \quad (33)$$

where  $\mathbf{D}$  is the differential operation matrix.

Final, the stiffness matrix,  $\mathbf{K}^p$ , for a single patch is also computed as,

$$\mathbf{K}^p = \iint_{\Omega} \mathbf{B}^T(\xi, \eta) \mathbf{C} \mathbf{B}(\xi, \eta) |J| \bar{t} d\xi d\eta \quad (34)$$

where  $\bar{t}$  is the thickness, , and  $\mathbf{J}$  is the jacobian matrix which maps the parametric space to the physical space.  $\mathbf{C}$  is the elastic material property matrix for plane stress.

In order to obtain the stiffness matrix and solve the integration i.e., Equation (34), the standard Gauss quadrature over each knot space is used for numerical integration. It is noted that the proper number of gauss points depends on the order of the NURBS basis functions.

## 6. TOPOLOGY OPTIMIZATION BASED ON BLSM WITH IGA

In this study, the BLSM with IGA is adopted for the topology optimization of plane structures. In fact, for analyzing plane structures in the topology optimization procedure the NURBS based-IGA is utilized instead of in the conventional FEM. In order to achieve purpose, in IGA control points are considered as nodes in FEM and B-Spline basis functions are utilized as shape functions of FEM for the analysis of structure. Boundary conditions are directly imposed on control points. The design model is also modeled using a fixed isogeometric mesh. Furthermore, the ‘‘Ersatz material’’ approach [16] is considered in this study in order to avoid the time-consuming re-meshing process of design model in the topology optimization procedure. Based on the ‘‘Ersatz material’’ approach, the elements

associated with the hole region are modeled by a weak material.

## 7. NUMERICAL EXAMPLE

In this section, three examples of plane elasticity structure are presented in order to demonstrate the performance of the topology optimization based on BLSM with IGSA. In all examples the modulus of elasticity, the Poisson's ratio and thickness are considered as  $1Pa$ ,  $0.3$  and  $0.01m$ , respectively. For modeling the hole in the analysis procedure of structures, the "Ersatz material" approach [16] is utilized. Based on this approach, the hole is filled by a weak material. For this purpose, Young's modulus of Ersatz material is assumed as  $10^{-3}Pa$ . The order of NURBS basis functions in each direction is equal to be 2.

### 7.1 Cantilever beam

The first problem is the cantilever beam shown in Fig. 1, which is a benchmark problem in topology optimization. As shown in Fig. 3, the length of the domain is  $L=80mm$  and the height is  $H=40mm$ . The cantilever beam is subjected to a concentrated load  $P=1N$  at the end point of the free end. The volume constraint is 40% of the total domain volume.

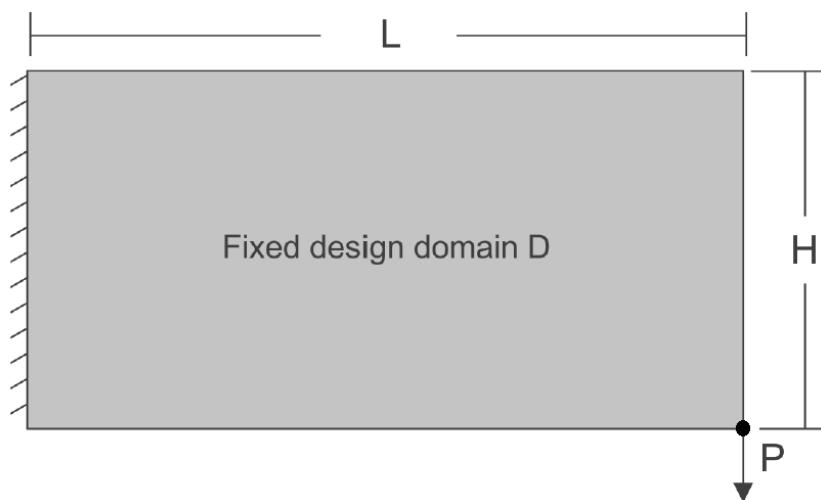


Figure 1. Fixed design domain and boundary condition of the cantilever beam

In this example, the initial geometry is modeled based on a bi-quadratic NURBS geometry with  $10 \times 6$  control points. The open knot vectors are respectively  $\{0, 0, 0, 0.125, 0.25, 0.375, 0.5, 0.625, 0.75, 0.875, 1, 1, 1\}$  and  $\{0, 0, 0, 0.25, 0.5, 0.75, 1, 1, 1\}$  in  $\xi$  and  $\eta$  direction, thus leading to  $8 \times 4$  knot spans. By subdividing each knot span into 10 equal parts in  $\xi$  and  $\eta$  direction, the physical mesh with  $80 \times 40$  knot spans and the control mesh with  $82 \times 42$  control points are obtained. In the BLSM, the time step size is  $t = 8$  and other parameters are assumed as  $\beta = 10^{-4}$ ,  $\mu_1 = 45$ ,  $\mu_2 = 450$  and  $\alpha = 0.95$ .

The evolution procedure of structural topology based on the proposed method is shown from Figs. 2(a) to 2(h). The final topology of the cantilever beam is also depicted in Fig. 2(h).

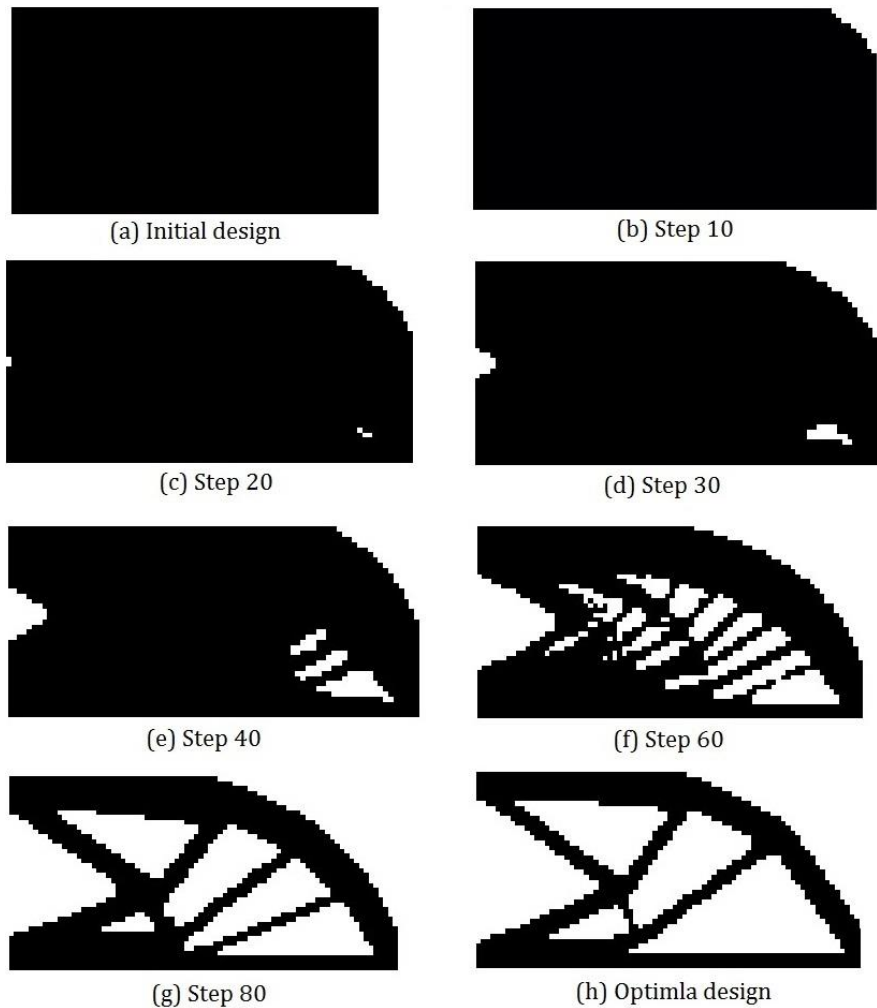
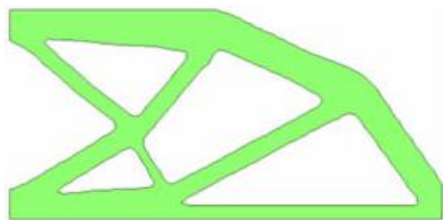
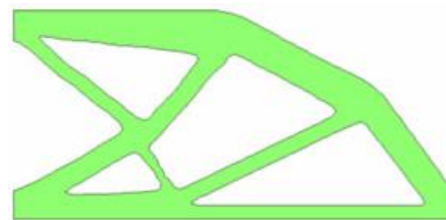


Figure 2. The evolution of the optimal topology for the cantilever beam

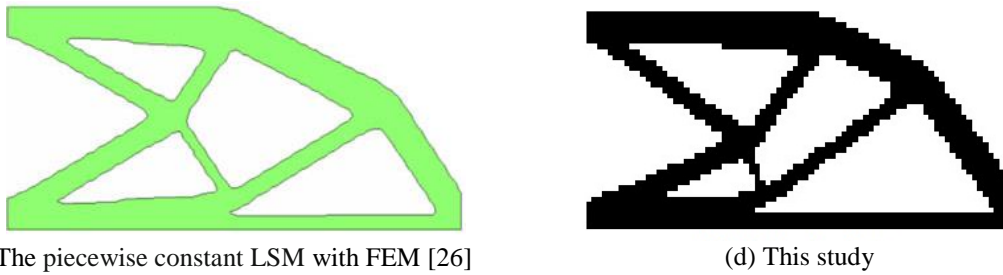
This example has been considered and investigated by other researchers. The final optimal topology obtained the proposed method of this study is compared with those obtained in the work of Shojaee and Moammadian [26] and shown in Fig. 3. It can be seen from Fig. 3 that the optimal design obtained in this study is similar to those reported in the literature.



(a) The AOS-MBO scheme with FEM [26]



(b) The MOS-MBO scheme with FEM [26]



(c) The piecewise constant LSM with FEM [26]

(d) This study

Figure 3. The comparison of the optimal topology in this study with that of Ref. [26]

The evolution of the compliance and the volume fraction are shown in Fig. 4. The value of the compliance at the optimal design is 82.6.

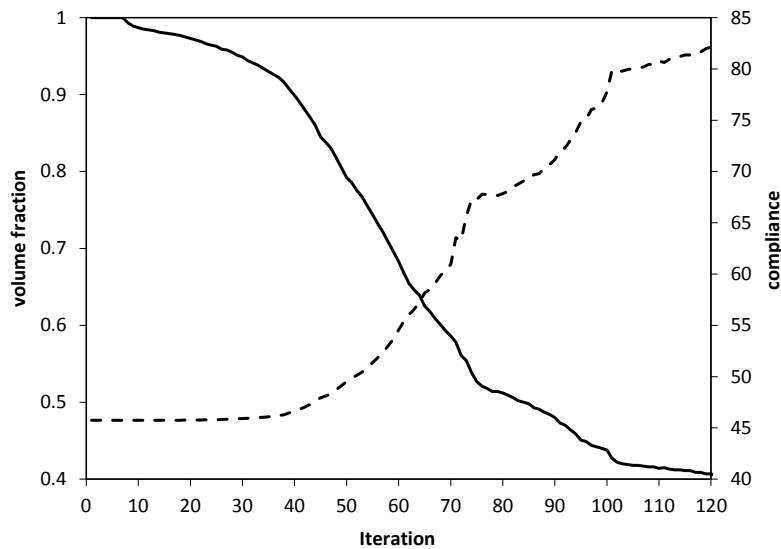


Figure 4. The convergence histories of the compliance and the volume ratio

### 7.2 Messerschmitt–Bölkow–Blom beam

Messerschmitt–Bölkow–Blom (MBB) beam considered as the second example is the benchmark problem for the topology optimization. The geometry model and loading conditions of the MBB beam is shown in Fig. 5. The length of the domain is  $L=120\text{mm}$  and the height is  $H=30\text{mm}$ . The problem is subjected to a concentrated load  $P=1\text{N}$  at the upper half of the vane. In the optimization procedure, the specified material volume fraction is 40%. In the BLSM, the time step size is  $t=8$  and other parameters are assumed as  $\beta=10^{-4}$ ,  $\mu_1=50$ ,  $\mu_2=400$  and  $\alpha=0.95$ .

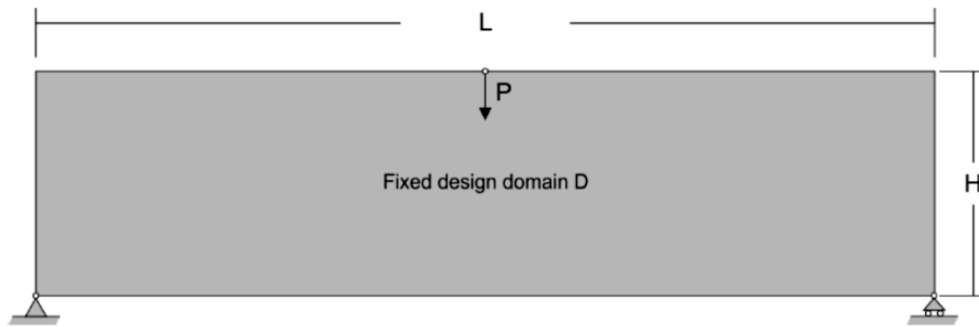


Figure 5. Fixed design domain and boundary condition of the MBB beam

In the first stage, the topology optimization is performed based on the proposed method with  $120 \times 30$  mesh isogeometric and the topology evolving history is depicted in Fig. 6. The optimal topology of the MBB beam is shown Fig. 6(h) which was obtained in the 92 iterations.

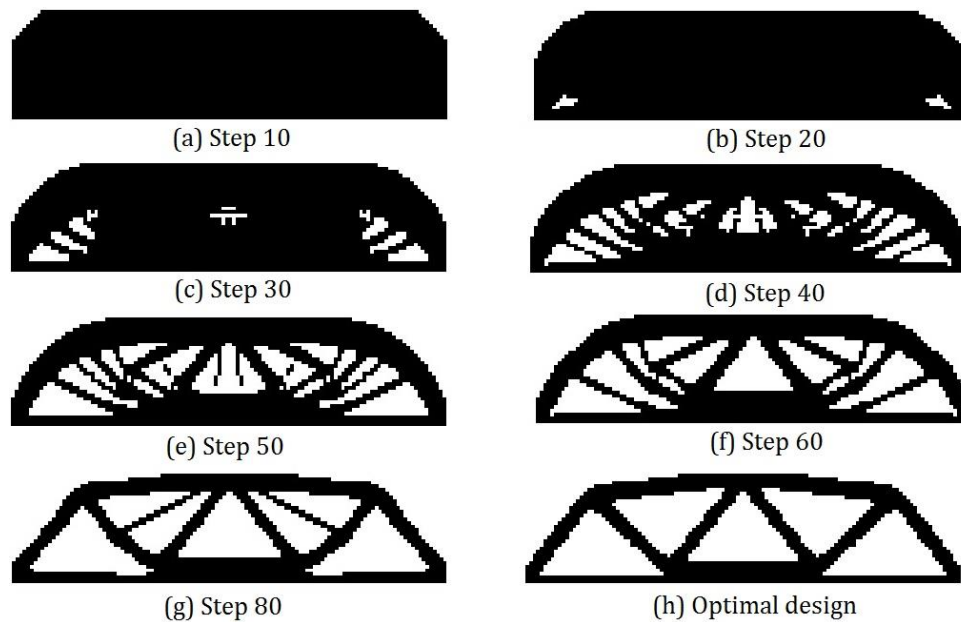


Figure 6. The evolution of the optimal topology for the MBB beam

In the work of Dai *et al.* [24], this example was investigated by a variational BLSM. The FEM was utilized for the analysis of the structure in the procedure of the topology optimization. The final optimal topology obtained in this study is compared with that obtained in the work of Dai *et al.* [24] and shown in Fig. 7. As can be seen from Fig. 7, the final design obtained in this study is similar to that reported in the literature.

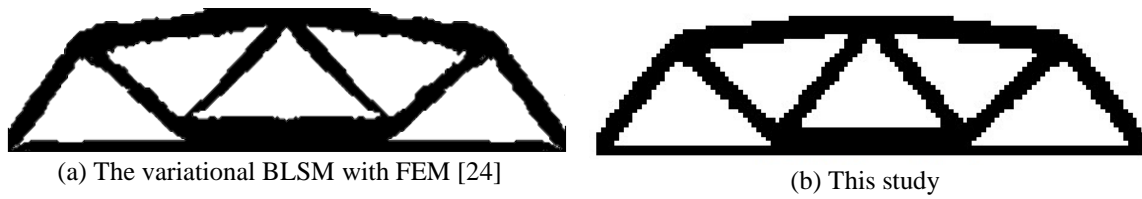


Figure 7. The comparison of the optimal topology in this study with that of Ref. [24]

Fig. 8 shows the structural strain energy variation history during the optimization process for the proposed method. In the figure the iteration history of material usage within the design domain during topology evolving is also depicted. The value of the compliance at the optimal design is 47.1.

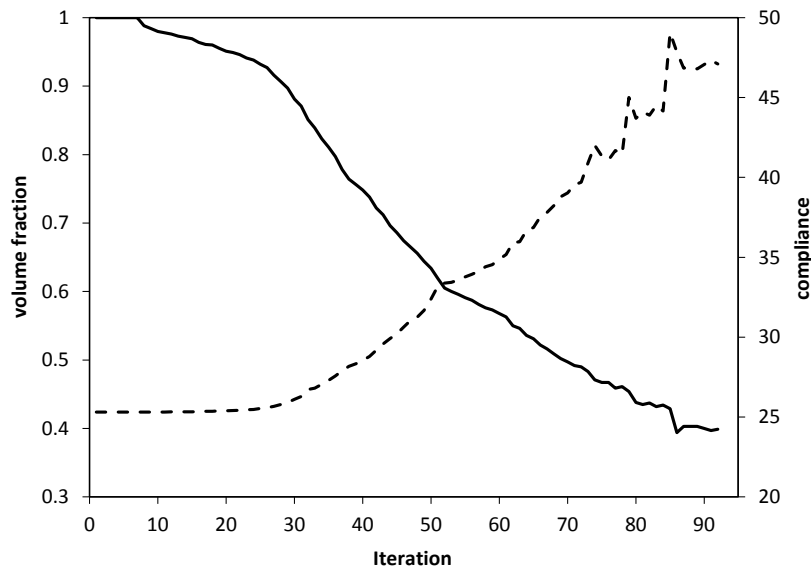


Figure 8. The convergence histories of the compliance and the volume ratio

### 7.3 Michell structure with multiple loads

The Michell type structure with multiple loads is considered as the final example. Fig. 9 shows the boundary condition of this kind of structure. The left corner of the bottom of the design domain is fixed and its right corner is simply supported. Three forces are applied at the equal spaced point at the bottom boundary with  $P_1 = 10N$  and  $P_2 = 5N$ . The design domain is  $80 \times 40$  which is discretized with 3200,  $1 \times 1$  squared elements. The volume fraction is chosen 40%. The BLSM is used for solving this problem without any holes in the initial design domain. The time step size is  $t = 8$  and other parameters are  $\beta = 10^{-4}$ ,  $\mu_1 = 45$ ,  $\mu_2 = 450$  and  $\alpha = 0.95$ .

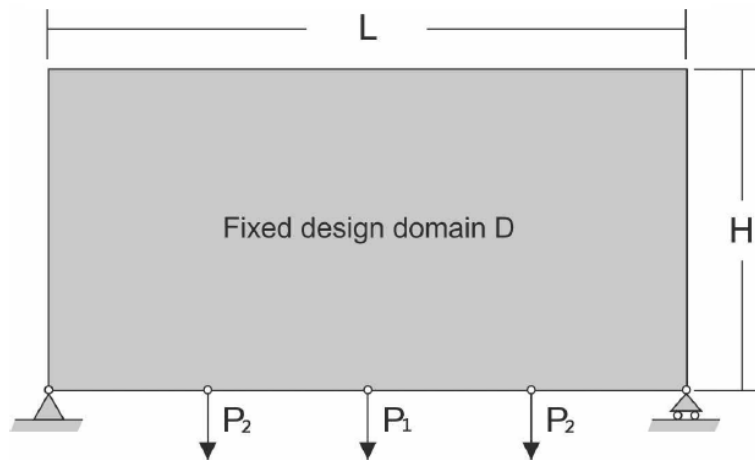


Figure 9. Fixed design domain and boundary condition of the Michell structure

The topology optimization is performed based on the proposed method and the topology evolving history is depicted in Fig. 10.

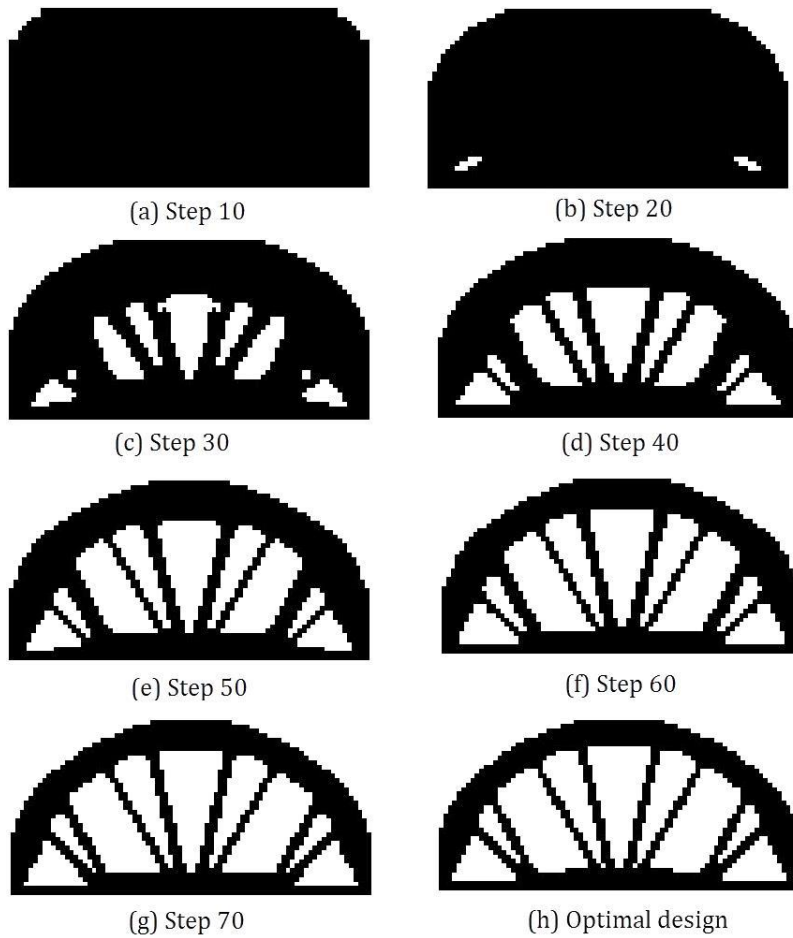


Figure 10. The evolution of the optimal topology for the Michell beam

The topology evolving history shows that the final topology is obtained in the 69 iterations. In the work of Shojaee and Moahmmadian [17], this example was investigated using the BLSM with FEM. The final optimal topology obtained in this study is compared with that obtained in the work of Shojaee and Moahmmadian [17] and shown in Fig. 11. As obvious from Fig. 11, the final design obtained in this study is similar to that reported in the literature.

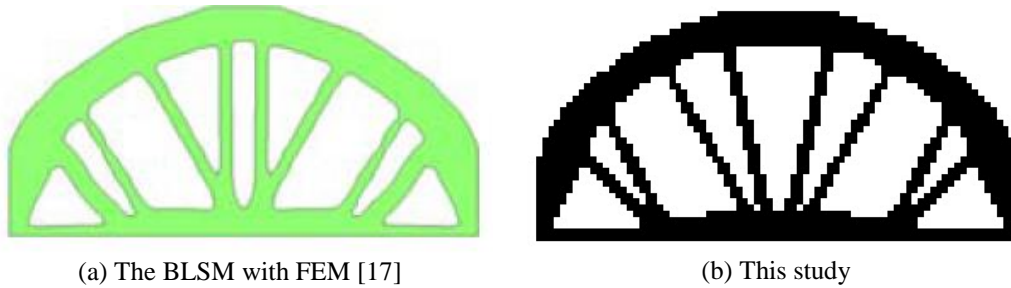


Figure 11. The comparison of the optimal topology in this study with that of Ref. [17]

It can be concluded from Fig. 11 that the optimal design obtained based on the IGA is similar to that of FEM. Fig. 12 shows the structural strain energy variation history during optimization for the proposed method. In the figure the iteration history of material usage within the design domain during topology evolving is also depicted. The value of the compliance at the optimal design is 4611.71.

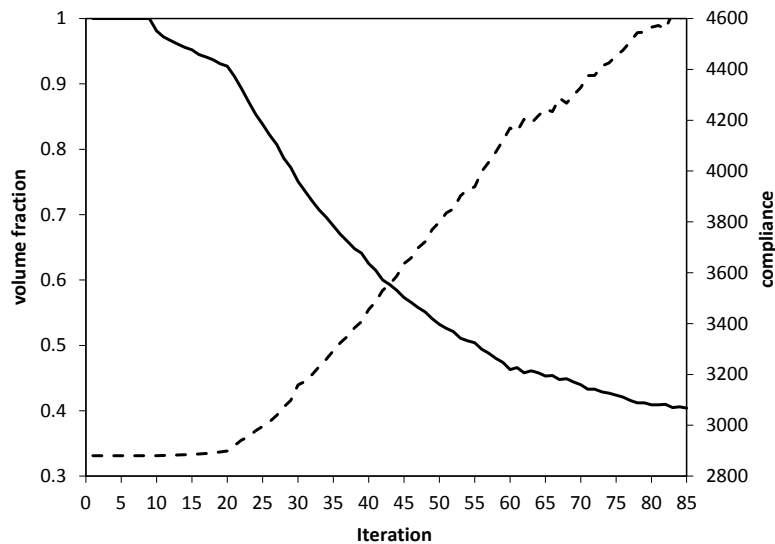


Figure 12. The convergence histories of the compliance and the volume ratio

## 8. CONCLUSIONS

This paper proposes the topology optimization of plane structures using the BLSM with IGA. The BLSM has the same advantage as the piecewise constant method. It does not need



to re-initialize level set function and can easily create small holes without topological derivatives during the evolution. This means that the BLSM can substantially reduce the computational complexity. In the topology optimization procedure the NURBS based-IGA approach is also utilized instead of in the conventional FEM.

The performance and capability of the BLS schemes with IGA is shown through the benchmark examples widely used in topology optimization. The final topology obtained by the proposed method are compared with outcome of topology optimization based on the other LSM techniques, and the results show similar topologies. Therefore, the optimization results demonstrate that this method can efficiently be used in the structural topology optimization.

## REFERENCES

1. Dijk NP, Maute K, Langelaar M, Keulen F. Level-set methods for structural topology optimization: a review, *Struct Multidisc Optim* 2013; **48**: 437-72.
2. Bendsoe MP, Sigmund O. *Topology Optimization: Theory, Methods, and Applications*, Springer, Berlin, 2003.
3. Bendsoe MP, Kikuchi N. Generating optimal topologies in structural design using a homogenization method, *Comput Methods Appl Mech Engrg* 1988; **71**: 97-224.
4. Rozvany GIN. *Structural Design via Optimality Criteria*, Kluwer Academic Publishers, Dordrecht, 1989.
5. Rozvany GIN, Zhou M. The COC algorithm, Part I: Cross section optimization or sizing, *Comput Meth Appl Mech Eng* 1991; **89**: 281-308.
6. Schmit LA, Farsi B. Some approximation concepts for structural synthesis, *AIAA J* 1974; **12**(5): 692-99.
7. Schmit LA, Miura H. *Approximation Concepts for Efficient Structural Synthesis*, NASA Publisher, Washington, United States, 1976.
8. Vanderplaats GN, Salajegheh E. A new approximation method for stress constraints in structural synthesis, *AIAA J* 1989; **27**(3): 352-58.
9. Svanberg K. The method of moving asymptotes—a new method for structural optimization, *Int J Numer Meth Eng* 1987; **24**: 359-73.
10. Tavakkoli SM, Hassani B, Ghasemnejad H. Isogeometric topology optimization of structures by using MMA, *Int J Optim Civ Eng* 2013; **3**: 313-26.
11. Kazemi HS, Tavakkoli SM, Naderi R. Isogeometric topology optimization of structures considering weight minimization and local stress constraints, *Int J Optim Civil Eng* 2016; **6**(2): 303-17.
12. Xie YM, Steven GP. A simple evolutionary procedure for structural optimization, *Comput Struct* 1993; **49**(5): 885-96.
13. Jakiela MJ, Chapman C, Duda J, Adewuya A, Saitou K. Continuum structural topology design with genetic algorithms, *Comput Meth Appl Mech Eng* 2000; **186**: 339-56.
14. Kaveh A, Hassani B, Shojaee S, Tavakkoli SM. Structural topology optimization using ant colony methodology, *Eng Struct* 2008; **30**(9): 2559-65.
15. Osher S, Sethian JA. Front propagating with curvature dependent speed: algorithms based on Hamilton-Jacobi formulations, *J Comput Phys* 1988; **78**: 12-49.

16. Allaire G, Jouve F, Toader AM. Structural optimization using sensitivity analysis and a level set method, *J Comput Phys* 2004; **194**: 363–93.
17. Shojaee S, Mohamadian M, A Binary Level Set Method for Structural Topology Optimization, *Int J Optim Civil Eng* 2011; **1**(1): 73–90.
18. Shojaee S, Mohamadian M, Valizadeh N. Composition of isogeometric analysis with level set method for structural topology optimization, *Int J Optim Civil Eng* 2012; **2**(1): 47–70.
19. Shojaee S, Mohaghegh A, Haeri A. Piecewise constant level set method based finite element analysis for structural topology optimization using phase field method, *Int J Optim Civil Eng* 2015; **5**(4): 389–407.
20. Roodsarabi M, Khatibinia M, Sarafrazi SR. Isogeometric topology optimization of structures using level set method incorporating sensitivity analysis, *Int J Optim Civil Eng* 2016; **6**(3): 405–22.
21. Roodsarabi M, Khatibinia M, Sarafrazi SR. Hybrid of topological derivative–based level set method and isogeometric analysis for structural topology optimization, *Steel Compos Struct* 2016; **21**(6): 1389–410.
22. Lie J, Lysaker M, Tai XC. A binary level set model and some applications to Mumford–Shah image segmentation, *IEEE Trans Image Process* 2006; **15**: 1171–81.
23. Tai XC, Christiansen O. Image segmentation using some piecewise constant level set methods with MBO type of projection, *Int J Comp Vis* 2007; **73**: 61–76.
24. Dai X, Tang P, Cheng X and Wu M. A variational binary level set method for structural topology optimization, *Commun Comput Phys* 13; **5**: 1292–308.
25. Tai XC, Christiansen O, Lin P and Skjævelaen I. Image segmentation using some piecewise constant level set methods with MBO type of projection, *Int J Comput Vis* 2007; **73**: 61–76.
26. Shojaee S and Mohammadian M. Piecewise constant level set method for structural topology optimization with MBO type of projection, *Struct Multidisc Optim* 2011; **44**: 455–69.
27. Hughes TJR, Cottrell J, Bazilevs Y. Isogeometric analysis: CAD, finite elements, NURBS, exact geometry and mesh refinement, *Comput Methods Appl Mech Engrg* 2005; **194**: 4135–95.
28. Xia Q, Shi T, Liu S, Wang MY. A level set solution to the stress–based structural shape and topology optimization, *Comput Struct* 2012; **90–91**: 55–64.
29. Wang M, Wang XM, Guo DM. A level set method for structural topology optimization, *Comput Methods Appl Mech Engrg* 2003; **192**: 227–46.
30. Osher S, Fedkiw R. *Level Set Methods and Dynamic Implicit Surfaces*, Springer, 2002.
31. Wang XM, Wang MY, Guo DM. Structural shape and topology optimization in a level–set framework of region representation, *Struct Multidisc Optim* 2004, **27**(1–2), 1–19.
32. Wei P, Wang MY. Piecewise constant level set method for structural topology optimization, *Int J Numer Meth Eng* 2009; **78**: 379–402.
33. Lu T, Neittaanmaki T, Tai XC. A parallel splitting up method and its application to Navier–Stokes equations, *Appl Math Lett* 1991; **4**: 25–9.
34. Weickert J, Romeny BM, Viergever M. Efficient and reliable schemes for nonlinear diffusion filtering, *IEEE Trans Image Processing* 1998; **7**: 398–410.